Ultracold atomic mode splitter for the entanglement of separated atomic samples

C. V. Chianca and M. K. Olsen
School of Mathematics and Physics, University of Queensland, Brisbane QLD 4072, Australia
(Received 11 June 2015; published 27 October 2015)

We propose and analyze the use of a three-well Bose-Hubbard model for the creation of two spatially separated entangled atomic samples. Our three wells are in a linear configuration, with all atoms initially in the middle well, which gives some spatial separation of the two end wells. The evolution from the initial quantum state allows for the development of entanglement between the atomic modes in the two end wells. We show how the detected entanglement and the well occupations are time dependent. We propose a method for preserving the entanglement by turning off the different interactions when it reaches its first maximum. We analyze the system with both Fock and coherent initial states, showing that the violations of the chosen inequality exist only for initial Fock states and that the collisional nonlinearity degrades them. This system is a preliminary step towards producing entangled atomic samples that can be spatially separated using recently developed methods of potential manipulation and thus help close the locality loophole in tests of quantum mechanics.

DOI: 10.1103/PhysRevA.92.043626 PACS number(s): 03.75.Gg, 03.67.Mn, 03.75.Lm, 67.85.Hj

I. INTRODUCTION

We propose a method for the fabrication of spatially separated entangled atomic populations, outlining a device which uses condensed atoms trapped in a three-well potential. For our parameters, this has a description in terms of the Bose-Hubbard model [1]. Shortly after the first trapped Bose-Einstein condensates (BECs), Jaksch *et al.* [2] showed that this model can provide an accurate description of bosonic atoms trapped in a deep optical lattice. In this work we use a three-well model to propose and analyze how to split an initial condensate in the central well into two separated entangled condensates. We then show how this entanglement may be preserved and make a suggestion for further spatial separation of the two parts of the bipartite entangled state, using recently developed methods of dynamic potential fabrication [3].

Continuous-variable entanglement is an area of active research [4,5], and includes the study of entanglement between bosonic fields, with a number of inequalities having been developed to detect the existence of this property. The most commonly used are those developed by Duan *et al.* [6] and Simon [7], using combinations of quadrature variances, which are suitable for quantum optical systems. The criteria we use here were developed by Hillery and Zubairy [8] and expanded on by Cavalcanti *et al.* [9] to cover multipartite entanglement, steering, and violations of Bell inequalities. As shown by He *et al.* [10], these criteria are well suited to number conserving processes, such as the present one.

Entanglement in condensed atomic systems has been predicted and examined in the processes of molecular dissociation [11], four-wave mixing [12–14], and in the Bose-Hubbard model [15]. In the latter, the tunneling between wells is a necessary but not sufficient condition for the existence of entanglement. Both the continuous [10,16,17] and pulsed tunneling configurations [18,19] have previously been treated. The correlations necessary to detect entanglement can in principle be measured using the interaction with light [20,21], or by homodyning with other atomic modes [22]. We note here that the entanglement we are examining is a collective property between atomic modes which are spatially separated, and is not between individual atoms [13]. This point, unavoidable for indistinguishable bosons, was recently put on a formal basis by Killoran *et al.* [23].

II. PHYSICAL MODEL, HAMILTONIAN AND EQUATIONS OF MOTION

In this article we will follow the approach taken by Milburn *et al.* [24], generalizng this to three wells [25,26], and using the fully quantum positive-P phase space representation [27]. We consider this to be the most suitable approach here because the equations are exact, it allows for an easy representation of mesoscopic numbers of atoms, it can be used to calculate quantum correlations, and it can simulate different quantum initial states [28]. Just as importantly, the positive-P calculations scale linearly with the number of sites and can in principle deal with any number of atoms. One disadvantage of the positive-P representation is that the integration can show a tendency to diverge at short times for high collisional nonlinearities [29], but the system under consideration is not in this regime. As long as the procedures followed to derive the Fokker-Planck equation for the positive-P function are valid [30], the stochastic solutions are guaranteed to be accurate wherever the integration converges. With all the results shown here, the solutions were found without any signs of divergences, and the sampling errors were smaller than the widths of the plotted lines.

The system is simple, with three potential wells in a linear configuration. Each of these contains a single atomic mode, which we treat as being in the lowest energy level. Atoms in each of the wells can tunnel into the nearest-neighbor potential; that is, between wells 1 and 2 and between wells 2 and 3. With all the population initially in the middle well, the system acts as a periodic mode splitter and recombiner. With the $\hat{a}_j$ as bosonic annihilation operators for atoms in mode j, J representing the coupling between the wells, and χ as the collisional nonlinearity, we may write our Hamiltonian. Following the usual procedures [24], we find

$$\mathcal{H} = \hbar \sum_{j=1}^{3} \chi \hat{a}_j^{\dagger 2} \hat{a}_j^2 - \hbar J(\hat{a}_1^\dagger \hat{a}_2 + \hat{a}_2^\dagger \hat{a}_1 + \hat{a}_3^\dagger \hat{a}_2 + \hat{a}_2^\dagger \hat{a}_3). \quad (1)$$

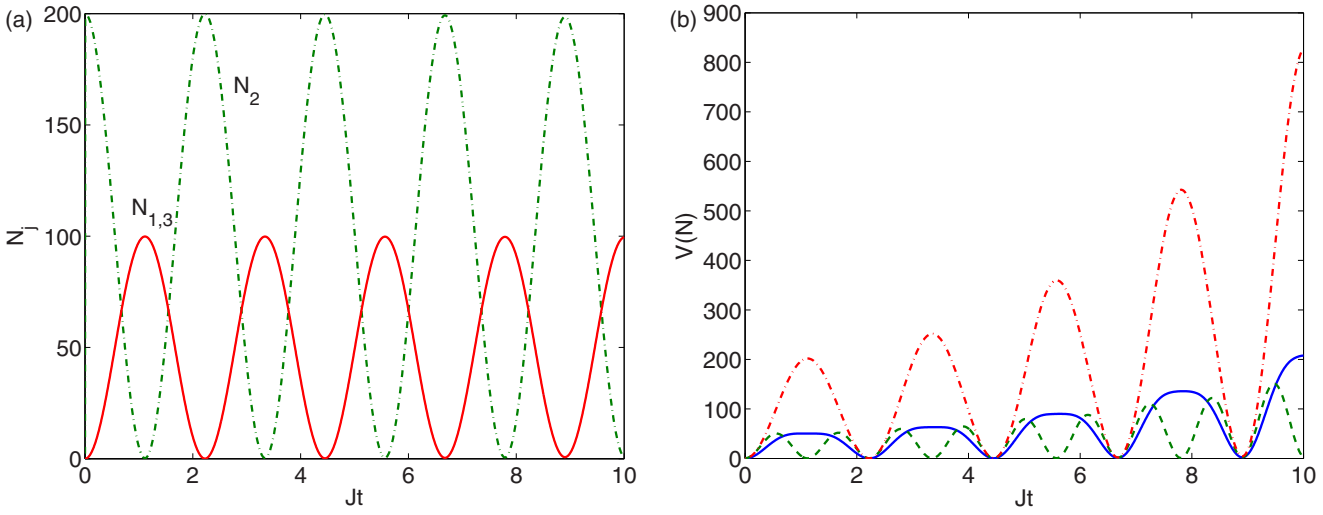

FIG. 1. (Color online) (a) The populations in each well as a function of time are shown on the left, for $J = 1$, $\chi = 10^{-3}$, and $N_2(0) = 200$, with $N_1(0) = N_3(0) = 0$. The atoms in the center well begin in a Fock state, although an initial coherent state leads to indistinguishable results. The quantities plotted in this and subsequent plots are dimensionless. (b) The number variances for the same parameters are shown in (a), and an initial Fock state. The solid line is $V(N_1)$, the dashed line is $V(N_2)$, and the dash-dotted line is $V(N_1 - N_3)$. We see that the variances are periodic and that the maximum variances increase with time.

We note here that the conditions of validity for this approach are given in Milburn *et al.* [24], and our atom numbers and nonlinearity are well within the regime where it is valid.

To solve the full quantum equations, we use stochastic integration of the positive-P representation [27], which are an exact mapping from the Hamiltonian of Eq. (1). Following the standard methods [31], the set of Itô stochastic differential equations [30] are found as

$$\begin{aligned}
\frac{d\alpha_1}{dt} &= -2i\chi\alpha_1^+\alpha_1^2 + iJ\alpha_2 + \sqrt{-2i\chi\alpha_1^2}\,\eta_1,\\
\frac{d\alpha_1^+}{dt} &= 2i\chi\alpha_1^{+2}\alpha_1 - iJ\alpha_2^+ + \sqrt{2i\chi\alpha_1^{+2}}\,\eta_2,\\
\frac{d\alpha_2}{dt} &= -2i\chi\alpha_2^+\alpha_2^2 + iJ(\alpha_1+\alpha_3) + \sqrt{-2i\chi\alpha_2^2}\,\eta_3,\\
\frac{d\alpha_2^+}{dt} &= 2i\chi\alpha_2^{+2}\alpha_2 - iJ(\alpha_1^+ + \alpha_3^+) + \sqrt{2i\chi\alpha_2^{+2}}\,\eta_4,\\
\frac{d\alpha_3}{dt} &= -2i\chi\alpha_3^+\alpha_3^2 + iJ\alpha_2 + \sqrt{-2i\chi\alpha_3^2}\,\eta_5,\\
\frac{d\alpha_3^+}{dt} &= 2i\chi\alpha_3^{+2}\alpha_3 - iJ\alpha_2^+ + \sqrt{2i\chi\alpha_3^{+2}}\,\eta_6,
\end{aligned} \tag{2}$$

where the η_j are standard Gaussian noises with $\overline{\eta_j} = 0$ and $\overline{\eta_j(t)\eta_k(t')} = \delta_{jk}\delta(t-t')$. As always, averages of the positive-P variables represent normally ordered operator moments, such that, for example, $\overline{\alpha_j^m\alpha_k^{+n}} \to \langle \hat{a}^{\dagger n}\hat{a}^m\rangle$. We note that, while $\overline{\alpha_j} = \overline{(\alpha_j^+)}^*$, $\alpha_j^* \neq \alpha_j^+$ on individual trajectories, and it is this freedom that allows classical variables to represent quantum operators.

The populations in each well are shown in Fig. 1(a), for $J = 1$, $\chi = 10^{-3}$, and $N_2(0) = 200$, with $N_1(0) = N_3(0) = 0$. We also calculate two types of quantum correlations. The first class of correlations are the number variances including the number difference between the populations of wells 1 and 3, shown in Fig. 1(b). In the positive-P formulation, these are written as

$$\begin{aligned}
V(N_j) &= \overline{\alpha_j^{+2}\alpha_j^2} + \overline{\alpha_j^+\alpha_j} - \overline{\alpha_j^+\alpha_j}^2,\\
V(N_1 - N_3) &= V(N_1) + V(N_3) - 2V(N1,N3),\\
&= V(N_1) + V(N_3)\\
&\quad - 2(\overline{\alpha_1^\dagger\alpha_1\alpha_3^\dagger\alpha_3} - \overline{\alpha_1^+\alpha_1}\times\overline{\alpha_3^+\alpha_3}),
\end{aligned} \tag{3}$$

with these all giving values of zero for uncorrelated Fock states. Whenever one of the variances is less than the mean population of that mode, we have suppression of number fluctuations below the coherent state level, which can be seen by comparison of the populations and variances shown in Fig. 1.

The second correlation is an entanglement measure adapted from an inequality developed by Hillery and Zubairy, who showed that, considering two separable modes denoted by i and j [8],

$$|\langle \hat{a}_i^\dagger\hat{a}_j\rangle|^2 \leqslant \langle \hat{a}_i^\dagger\hat{a}_i\hat{a}_j^\dagger\hat{a}_j\rangle, \tag{4}$$

with the equality holding for coherent states. The violation of this inequality is thus an indication of the inseparability of, and entanglement between, the two modes. Cavalcanti *et al.* [9] have extended this inequality to provide indicators of Einstein-Podolsky-Rosen (EPR) steering [32–34] and Bell violations [35]. We now define the correlation function

$$\xi_{13} = \langle \hat{a}_1^\dagger\hat{a}_3\rangle\langle \hat{a}_1\hat{a}_3^\dagger\rangle - \langle \hat{a}_1^\dagger\hat{a}_1\hat{a}_3^\dagger\hat{a}_3\rangle, \tag{5}$$

for which a positive value reveals entanglement between modes 1 and 3. We easily see that ξ_{13} gives a value of zero for two independent coherent states and a negative result for two independent Fock states. This inequality, and the EPR steering development of it, have been shown to detect both inseparability and asymmetric steering in a three-well

Bose-Hubbard model under the process of coherent transfer of atomic population (CTAP) [18,19].

III. RESULTS

In all the results presented here, we begin with 200 atoms in the middle well, with the other two being empty. We begin with these atoms initially in either Fock or coherent states, modeled as in Ref. [28]. We note that this allows us to sample the appropriate positive-P distributions for these states using the Gaussian random number generator found in Matlab, for example. The equations were numerically integrated over sufficient numbers of stochastic trajectories that the sampling errors became insignificant. These numbers, while different each time we ran our program, were always of the order of one million. We found that an initial coherent state gave the same average populations in each well as for a Fock state, but no entanglement was found according to the measure of Eq. (5), and independently of the nonlinearity used.

The populations of each well as a function of scaled time Jt are shown in Fig. 1. As expected, we see that the average populations of wells 1 and 3 are identical. We also see that the oscillations are highly regular over the time investigated, with no sign of the damping of oscillations seen in other Bose-Hubbard systems [24,26]. While this will happen for higher collisional nonlinearities, these also degrade the entanglement. On this scale, the results for $\chi = 0$ are indistinguishable from those for $\chi = 10^{-5}$. In Fig. 1(b) we show the number variances for the quantities N_1 ($=\hat{a}_1^\dagger \hat{a}_1$), N_2, and $N_1 - N_3$, the population difference between the two initially empty wells. As the tunneling Hamiltonian is analogous to that of a beamsplitter, we do not expect the interaction to produce any squeezing such as would be expected from pair production. Consistent with this, we see that all the variances, while oscillatory, evolve under an envelope which increases with time. The number variance of a coherent state is equal to the mean number, and the individual variances for N_1 and N_2 stay below this level for some time, while the variance in the population difference $N_1 - N_3$ has risen above this level by the second oscillation. This shows that the tunneling adds noise to the system, which is to be expected because the tunneling in each direction is independent. At the level of individual particles, the tunneling in each direction is random, so that any initial sub-Poissonian statistics will evolve toward being Poissonian and then super-Poissonian.

We now turn to the calculation of ξ_{13} of Eq. (5), our chosen entanglement witness. For initial coherent states we found no evidence of entanglement at all, independent of the strength of the χ nonlinearity. This is consistent with our previous result for coherent population transfer [19], where entanglement was also not found for an initial coherent state. When we consider an initial Fock state of fixed number, we do find evidence of entanglement, as shown in Fig. 2. We investigated three different positive values of χ, finding that the stronger interactions tend to degrade the predicted entanglement as time increases. For nonlinearites $\chi = 10^{-4}$ and 10^{-5} we see that the signature of the entanglement is periodic, with no sign of degradation up to $Jt = 10$. On the other hand, with $\chi = 10^{-3}$, the function stays negative after three oscillations, with the first peak being noticeably higher than the other two.

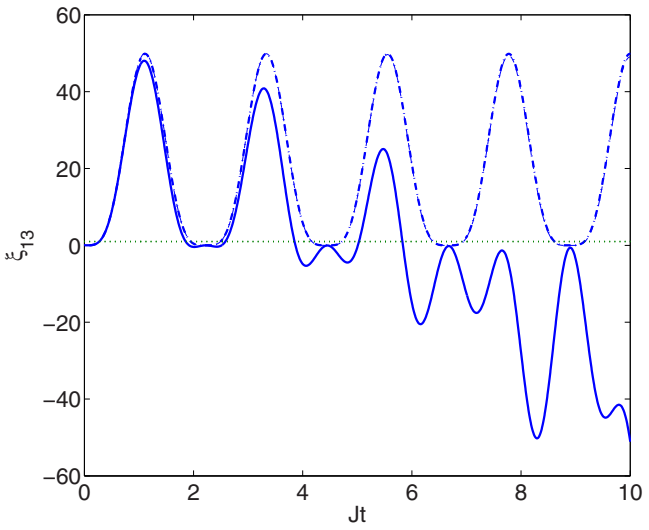

FIG. 2. (Color online) The entanglement criteria, ξ_{13}, as a function of time, for $J = 1$ and an initial Fock state in the middle well. The solid line is for $\chi = 10^{-3}$, while the almost indistinguishable dashed and dashed-dotted lines are for $\chi = 10^{-4}$ and $\chi = 10^{-5}$. We see that the entanglement is more persistent for lower nonlinearities. The line at zero is a guide to the eye.

We also calculated the EPR steering extension of ξ_{13}, but found no positive values for any times or nonlinearities, indicating that the degree of inseparability produced is not sufficient for a demonstration of this property.

The nonlinear interaction, known from previous work to produce squeezing [36] and non-Gaussian entanglement and EPR steering [37], degrades the chosen quantum correlations in this system. In the nonlinear coupler [38], comprising two evanescently coupled Kerr waveguides in an optical cavity, the nonlinearity creates the necessary quantum states since the cavity is pumped with a coherent input. The difference from the present system is that the nonlinearity is smaller and both interactions have many cavity lifetimes to create the quantum correlations. In quantum optics, as illustrated in Ref. [37], one simple method of obtaining entanglement is to put a coherent state through a nonlinear interaction so as to produce a quantum state of the electromagnetic field, such as a squeezed state. This can then be mixed on a beamsplitter, either with vacuum or another quantum state, with the outputs being entangled [39]. That this does not happen with our model when starting from a coherent state indicates that the collisional nonlinearity does not have time to form a sufficiently quantum state before the tunneling takes effect.

Two methods suggest themselves to surmount this difficulty with our system. We can either hold the middle well isolated until the nonlinearity has acted sufficiently to form an appropriate quantum state, or turn the tunneling off at the first maximum of population transfer. Because we do not know *a priori* how long a sufficiently squeezed state will take to develop, we do not investigate this option here. We will instead use the freedom in engineering optical potentials that is being developed at the present time [3] and assume that the two end wells can be changed and moved at the time of the first maximum of population transfer, which is also the time of

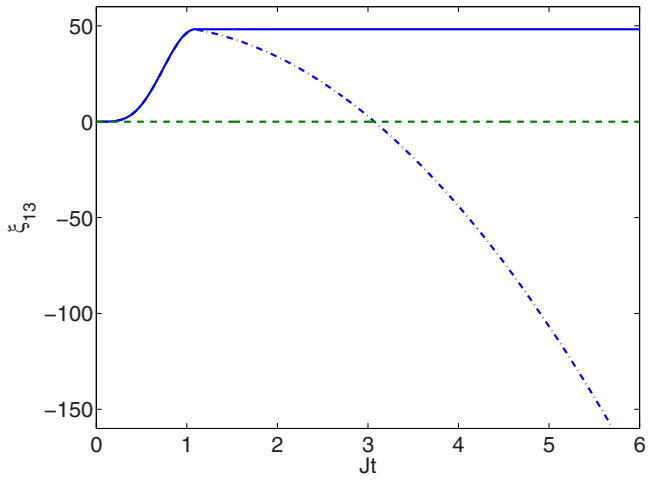

FIG. 3. (Color online) The entanglement criteria, ξ_{13}, as a function of time, for pulsed tunneling, with $J = 1$ turned off at $t = \tau_p$ ($\approx$1.1), the first time of maximum population transfer. The solid line is for $\chi = 10^{-3}$ also turned off at time τ_p, while the dashed-dotted line represents the evolution with χ constant. The line at zero is a guide to the eye. We see that the nonlinearity prevents this measure from registering entanglement after approximately one more of the oscillatory periods shown in Fig. 1.

the maximal entanglement signature. Labeling this time as τ_p, we use a time dependent $J(t) = 1 - \Theta(\tau_p)$, where Θ is the Heaviside step function. The results are shown in Fig. 3 as the dashed line, where we see that the entanglement signature begins to decay as soon as the tunneling is turned off. This suggests turning the nonlinear interaction off either at the same time as the tunneling, or even before the tunneling begins, possible in principle via Feshbach resonance techniques, with the result of this shown as the solid line. Without the scattering term, the value of ξ_{13} remains constant as we essentially have the free evolution of harmonic oscillators. We accept that these results are idealized, with the actual times needed to change the potentials and to initiate a Feshbach resonance depending on the experimental setup. Although our analysis here is not designed to model an actual experiment with all the attendant noise sources, it does point to a possible method for the achievement of spatially isolated entangled atomic samples. The techniques of Ref. [3] allow for the dynamical modification of optical potentials and thus further separation and isolation of the two occupied wells. This may be a small initial step towards the objective of being able to do measurements on each well within the time it would take for a signal to pass between them.

IV. CONCLUSIONS AND DISCUSSION

In conclusion, we have proposed and analyzed a simple atomic entangling analog of a combined mode splitter and recombiner, showing that it can be used to manufacture spatially separated entangled atomic modes. This is a step towards removing the locality or communication loophole from tests of entanglement and EPR steering for massive bosons. We have performed a fully quantum analysis of our model, making no approximations in the actual calculations. Using an inequality suited to systems with number conservation, we have calculated the entanglement available, and shown how to preserve this by turning off the tunneling and collisional interactions. We have also shown that, in order to produce entangled modes by this method, having an initial state with quantum correlations is more important than the interactions. In fact, given an initial nonclassical state, the collisional nonlinearity only acts to degrade the performance. As a Fock state is the natural state of a single atomic mode of an isolated well, it is to our advantage that this state can be used to produce a clear entanglement signal. The exact reproduction of such a state for a series of experimental runs will depend on the ability of experimenters to create condensed samples with close to the same number of atoms. The conceptual simplicity of our system suggests that there should be no insurmountable barriers to an experimental realization.

ACKNOWLEDGMENTS

This research was supported by the Australian Research Council under the Future Fellowships Program (Grant ID FT100100515). We acknowledge fruitful discussions with Joel Corney, Simon Haine, and Mark Baker.

[1] H. Gersch and G. Knollman, Phys. Rev. **129**, 959 (1963).
[2] D. Jaksch, C. Bruder, J. I. Cirac, C. W. Gardiner, and P. Zoller, Phys. Rev. Lett. **81**, 3108 (1998).
[3] K. Henderson, C. Ryu, C. MacCormick, and M. G. Boshier, New J. Phys. **11**, 043030 (2009).
[4] S. L. Braunstein and P. van Loock, Rev. Mod. Phys. **77**, 513 (2005).
[5] C. Weedbrook, S. Pirandola, R. Garcia-Patrón, N. J. Cerf, T. C. Ralph, J. H. Shapiro, and S. Lloyd, Rev. Mod. Phys. **84**, 621 (2012).
[6] L.-M. Duan, G. Giedke, J. I. Cirac, and P. Zoller, Phys. Rev. Lett. **84**, 2722 (2000).
[7] R. Simon, Phys. Rev. Lett. **84**, 2726 (2000).
[8] M. Hillery and M. S. Zubairy, Phys. Rev. Lett. **96**, 050503 (2006).
[9] E. G. Cavalcanti, Q. Y. He, M. D. Reid, and H. M. Wiseman, Phys. Rev. A **84**, 032115 (2011).
[10] Q. Y. He, P. D. Drummond, M. K. Olsen, and M. D. Reid, Phys. Rev. A **86**, 023626 (2012).
[11] K. V. Kheruntsyan, M. K. Olsen, and P. D. Drummond, Phys. Rev. Lett. **95**, 150405 (2005).
[12] G. K. Campbell, J. Mun, M. Boyd, E. W. Streed, W. Ketterle, and D. E. Pritchard, Phys. Rev. Lett. **96**, 020406 (2006).
[13] M. K. Olsen and M. J. Davis, Phys. Rev. A **73**, 063618 (2006).
[14] A. J. Ferris, M. K. Olsen, and M. J. Davis, Phys. Rev. A **79**, 043634 (2009).
[15] A. P. Hines, R. H. McKenzie, and G. J. Milburn, Phys. Rev. A **67**, 013609 (2003).
[16] J. Estève, C. Gross, A. Welle, S. Giovanazzi, and M. K. Oberthaler, Nature (London) **455**, 1216 (2008).

[17] Q. Y. He, M. D. Reid, T. G. Vaughan, C. Gross, M. K. Oberthaler, and P. D. Drummond, Phys. Rev. Lett. **106**, 120405 (2011).
[18] M. K. Olsen, J. Phys. B **47**, 095301 (2014).
[19] M. K. Olsen, J. Opt. Soc. Am. B **32**, A15 (2015).
[20] J. F. Corney and G. J. Milburn, Phys. Rev. A **58**, 2399 (1998).
[21] A. S. Bradley, M. K. Olsen, S. A. Haine, and J. J. Hope, Phys. Rev. A **76**, 033603 (2007).
[22] A. J. Ferris, M. K. Olsen, E. G. Cavalcanti, and M. J. Davis, Phys. Rev. A **78**, 060104 (2008).
[23] N. Killoran, M. Cramer, and M. B. Plenio, Phys. Rev. Lett. **112**, 150501 (2014).
[24] G. J. Milburn, J. F. Corney, E. M. Wright, and D. F. Walls, Phys. Rev. A **55**, 4318 (1997).
[25] K. Nemoto, C. A. Holmes, G. J. Milburn, and W. J. Munro, Phys. Rev. A **63**, 013604 (2000).
[26] C. V. Chianca and M. K. Olsen, Phys. Rev. A **84**, 043636 (2011).
[27] P. D. Drummond and C. W. Gardiner, J. Phys. A **13**, 2353 (1980).
[28] M. K. Olsen and A. S. Bradley, Opt. Commun. **282**, 3924 (2009).
[29] M. J. Steel, M. K. Olsen, L. I. Plimak, P. D. Drummond, S. M. Tan, M. J. Collett, D. F. Walls, and R. Graham, Phys. Rev. A **58**, 4824 (1998).
[30] C. W. Gardiner, *Stochastic Methods: A Handbook for the Natural and Social Sciences* (Springer-Verlag, Berlin, 2002).
[31] D. F. Walls and G. J. Milburn, *Quantum Optics* (Springer-Verlag, Berlin, 1995).
[32] A. Einstein, B. Podolsky, and N. Rosen, Phys. Rev. **47**, 777 (1935).
[33] E. Schrödinger, Proc. Cambridge Philos. Soc. **31**, 555 (1935).
[34] H. M. Wiseman, S. J. Jones, and A. C. Doherty, Phys. Rev. Lett. **98**, 140402 (2007).
[35] J. S. Bell, *Speakable and Unspeakable in Quantum Mechanics* (Cambridge University Press, London, 1987).
[36] S. A. Haine and M. T. Johnsson, Phys. Rev. A **80**, 023611 (2009).
[37] M. K. Olsen and J. F. Corney, Phys. Rev. A **87**, 033839 (2013).
[38] M. K. Olsen, Phys. Rev. A **73**, 053806 (2006).
[39] T. Aoki, N. Takei, H. Yonezawa, K. Wakui, T. Hiraoka, A. Furusawa, and P. van Loock, Phys. Rev. Lett. **91**, 080404 (2003).